

## Structural Comparison of Self-Organized Adlayers of Ligands and Their Metal-Coordinated Complexes on a Au(111) Surface: An STM Study

Qun-Hui Yuan<sup>[a, b]</sup> and Li-Jun Wan<sup>\*[a]</sup>

**Abstract:** Scanning tunneling microscopy (STM) was employed to investigate the adsorption of the linear-spacer-bridged ligands bis(pyrrrol-2-yl-methyl-eneamine) (BPMB and BPMmB), and their Zn<sup>II</sup>-coordinated complexes, BPMB/Zn<sup>II</sup> and BPMmB/Zn<sup>II</sup>, onto a Au(111) surface in 0.1 M HClO<sub>4</sub> solution. Both the ligands, with different spacer bridges, and their Zn<sup>II</sup> com-

plexes adsorb onto the Au(111) surface and self-organize into highly ordered two-dimensional arrays. The complexes BPMB/Zn<sup>II</sup> and BPMmB/Zn<sup>II</sup> appear in helical and triangular conformations, respectively, consistent with their

chemical structures. Although the metal complexes include ligands, the assembled structures and adlayer symmetries of the ligands and complexes are totally different. The structures and intramolecular features obtained by high-resolution STM imaging are discussed. The results should be important in fabricating surface supramolecular structures.

**Keywords:** ligands • monolayers • self-assembly • STM • Zn

### Introduction

During the development of modern coordination chemistry, various metal–ligand complexes with elaborate structures have been synthesized.<sup>[1]</sup> The structural complexities as well as coordination processes of these metal–ligand complexes can be compared to those of biological systems formed by self-assembly with weak inter- or intramolecular interactions.<sup>[1b,j]</sup> These complexes with different shapes and geometries, from a simple planar-shaped rhomboid to higher symmetry polygon cages,<sup>[1]</sup> usually present interesting electronic, optical, and magnetic properties and show potential in the fabrication of nanometer-scale devices.<sup>[1b,e,2]</sup> One of the prerequisites for employing these molecules in nanotechnology is the construction of ordered and controllable molecular nanostructures on solid surfaces. For this purpose, the technique of self-assembly or self-organization has proven to be a powerful “bottom-up” approach for nanodevice fabrication. This technique is of great importance in chemistry and materials science, especially in the construction of molecular nanostructures on solid surfaces.<sup>[3]</sup> It is possible to obtain

structural information on various self-organization processes at atomic or submolecular scale by using the well-established scanning tunneling microscopy (STM) technique. This is one of the most powerful tools in surface or interfacial analysis and has been used to characterize surface molecular architectures in various environments.<sup>[4]</sup> Moreover, STM images can provide structural evidence of complicated supramolecules, enabling the molecular structures prepared by coordination chemists to be confirmed. For instance, the direct evidence of chemical structure in a complex of a calix[8]arene derivative with fullerene was provided by STM on a Au(111) surface, which showed clearly the configurations of calix[8]arene and C<sub>60</sub>.<sup>[5]</sup>

There has been increasing interest in the fabrication of metal-complex nanostructures by the self-assembly method.<sup>[3c,6]</sup> For example, Lehn et al. observed the variation of molecular orientations by changing substituents at given locations.<sup>[6a]</sup> The supramolecular assemblies were constructed on highly oriented pyrolytic graphite (HOPG) surfaces by using a bis(terpyridine) ligand. A (2 × 2) grid-type array of Zn<sup>II</sup> and Co<sup>II</sup> complexes was observed by STM.<sup>[6b]</sup> Kurth and Rabe et al. prepared perfectly straight nanostructures of metallosupramolecular coordination-polyelectrolyte amphiphile complexes on graphite surfaces.<sup>[6c]</sup> Wan and Stang et al. fabricated the mesoscopic self-organizations of a supramolecular rectangle on both HOPG and Au(111) surfaces.<sup>[3c]</sup> The rectangles spontaneously adsorb onto both surfaces and self-organize into well-ordered adlayers. On a HOPG surface, the long edge of the rectangle stands on the

[a] Q.-H. Yuan, Prof. Dr. L.-J. Wan  
Institute of Chemistry, Chinese Academy of Sciences (CAS)  
Beijing 100080 (China)  
Fax: (+86) 10-6255-8934  
E-mail: wanlijun@iccas.ac.cn

[b] Q.-H. Yuan  
Also in Graduate School of CAS, Beijing (China)

surface, forming a two-dimensional molecular network. In contrast, the face of the rectangle lies on the Au(111) surface in a flat-lying orientation, forming linear chains. This result implies that the interaction between molecule and substrate plays an important role in the formation of the different adlayers.

Although the metal–ligand complex includes ligand, the assembled structures of ligand and complex can be totally different. The adsorption behavior that a ligand and its complex will adopt on the same solid substrate is an interesting issue in surface chemistry, supramolecular chemistry, and nanostructure fabrication. Therefore, understanding the structural differences between the self-assemblies of ligand and its complex is important if they are to be employed as building blocks for surface molecular architectures. Until now, the structural relationship between a ligand and its complex in their self-organization on a solid surface has been rarely studied. Recently, Ma et al. synthesized several linear-spacer-bridged bis(pyrrol-2-yl-methyleneamine)s, which are ideal building blocks for fabricating supramolecular complexes with metal ions.<sup>[7]</sup> By varying the spacer bridges between two pyrrol-2-yl-methyleneamine units, the ligands can form complexes with Zn<sup>II</sup> ions in special shapes, such as a double-stranded helix and a triangle. The typical ligands used in this study are linear-spacer-bridged bis(pyrrol-2-yl-methyleneamine) (BPMB and BPMmB), and their Zn<sup>II</sup>-coordinated complexes, BPMB/Zn<sup>II</sup> and BPMmB/Zn<sup>II</sup>. The chemical structures and space-filling models of these ligands are shown in Scheme 1. Here, we employed these two

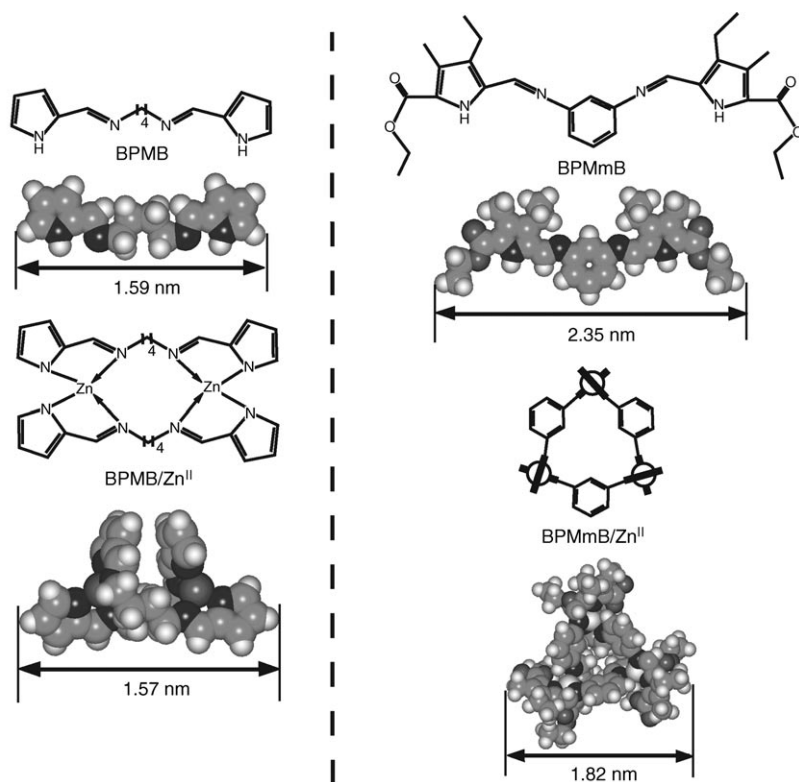
pairs of ligands and complexes to prepare adlayers on a Au(111) surface. The structural differences between the adlayers of ligands and complexes were investigated by STM. Both the ligands with different spacer bridges and their Zn<sup>II</sup> complexes can adsorb onto the Au(111) surface and self-organize into highly ordered two-dimensional arrays. Two complexes, BPMB/Zn<sup>II</sup> and BPMmB/Zn<sup>II</sup>, appear in helical and triangular conformations, respectively, and two ligands form a linear shape, consistent with their chemical structures. The adlayer symmetries are determined from STM images. This study provides structural information for determining the differences between self-organizations of ligands and their complexes.

## Results and Discussion

**BPMB ligand:** The self-assembly of ligand BPMB was investigated initially by STM. Figure 1a is a typical large-scale STM image of a BPMB adlayer recorded at 550 mV on Au(111) in 0.1 M HClO<sub>4</sub> solution. The ligands adsorb onto the Au(111) surface and self-organize into a long-range ordered adlayer. The molecules form ordered molecular rows along the *A* and *B* directions, which cross each other at an angle of 65° with an experimental error of ±2°. The molecular rows in the *A* direction are composed of regular sets of two bright spots.

The structural details of the ligand adlayer were studied by high-resolution STM imaging. Figure 1b is a high-resolution STM image of the area shown in Figure 1a. In Figure 1b, each ligand can be resolved as a dumbbell-shaped protrusion highlighted by a pair of ellipses.

The average length of each individual ligand was measured as 1.6 ± 0.1 nm, consistent with the optimized size of BPMB shown in Scheme 1. The insert in the lower left corner shows a single ligand and the two depressions of the ligand can be clearly seen. From the chemical structure of BPMB, the two bright spots with dark depressions in the center correspond to the two Schiff-base units of the molecule. Therefore, it can be concluded that the BPMB ligands are self-assembled on the Au(111) surface side-by-side in the *A* direction and form a well-ordered adlayer. Each ligand assumes a flat-lying orientation on the Au(111) lattice. The underlying Au(111) substrate lattice could also be observed in the



Scheme 1. Chemical structures and space-filling models of ligands BPMB and BPMmB, and their Zn<sup>II</sup> complexes BPMB/Zn<sup>II</sup> and BPMmB/Zn<sup>II</sup>.

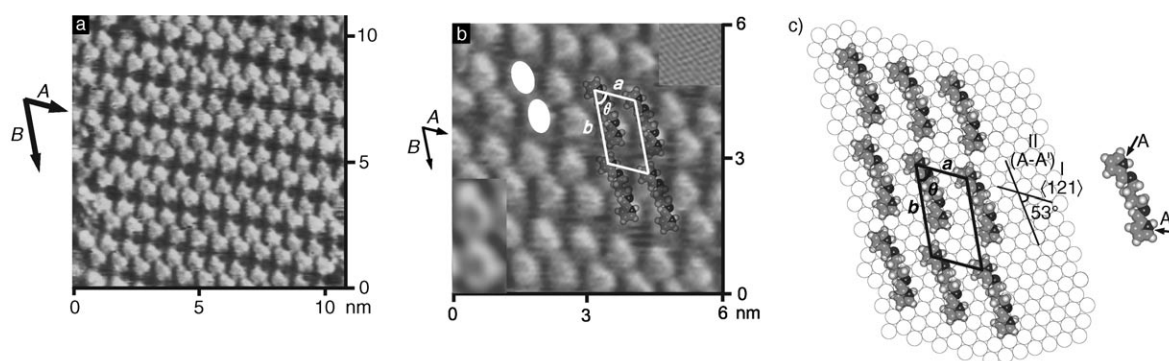


Figure 1. a) Large-scale STM image of BPMB ligands adsorbed onto Au(111). b) High-resolution STM image of the BPMB ligands in (a). Imaging conditions:  $E=550$  mV,  $E_{\text{tip}}=421$  mV,  $I_{\text{tip}}=2.11$  nA. The insert in the lower left corner of (b) shows a single BPMB molecule. The insert in the upper right corner shows an Au(111)-(1 × 1). c) Proposed structural model for the BPMB adlayer.

same experiment by scanning the electrode potential to the hydrogen-adsorption region, in which the ligand adlayer desorbed from the surface. The insert in the upper right corner in Figure 1b shows the substrate lattice. Comparison of the Au(111) substrate with the ligand molecular adlayer shows that the rows of BPMB ligands in the  $A$  direction are aligned along the  $\langle 121 \rangle$  direction of the underlying Au(111) lattice. From the adlayer symmetry, a unit cell could be deduced, as outlined in Figure 1b. In this unit cell, the intermolecular distances along two molecular rows were measured to be  $a=1.0\pm 0.1$  nm and  $b=1.8\pm 0.1$  nm. The angle  $\theta$  is  $65^\circ$ . It was observed that the direction of each ligand along its longer axis deviates by  $7^\circ$  from the  $\langle 121 \rangle$  direction of the Au(111) underlying lattice.

On the basis of the intermolecular distances and molecular orientation, a structural model for the adlayer is proposed in Figure 1c. The adlayer is defined as a  $(2\sqrt{3}\times\sqrt{37})$  structure. The  $A$  direction is rotated from the close-packed Au(111) direction by  $30^\circ$ , and the  $B$  direction is rotated by  $25^\circ$ . The molecules adsorb onto the Au(111) surface in a flat-lying orientation and form a well-defined assembly. To explain clearly the adsorption geometry, two markers  $A$  and  $A'$  were used to indicate two nitrogen atoms in pyrrole rings

of a BPMB ligand. The direction of each ligand along its longer axis  $A-A'$  deviates by around only  $7^\circ$  from the  $\langle 121 \rangle$  direction, consistent with the STM observations shown in Figure 1b. In this model, the pyrrole rings of Schiff-base units in each molecule sit on the three-fold positions of the underlying Au(111) lattice, which may be responsible for the  $7^\circ$  deviation of the ligand from the  $\langle 121 \rangle$  direction.

**BPMB/ $\text{Zn}^{\text{II}}$  complex:** We prepared an adlayer of the  $\text{Zn}^{\text{II}}$ -coordinated complex with BPMB ligands on Au(111). The adlayer structure was observed by employing STM. Figure 2a shows a typical large-scale STM image of complexes on Au(111). A highly ordered and consistent molecular array of the complexes was observed and the STM image was reproducible, although a reconstructed Au(111) surface with herringbone lines can be seen in the image. Molecular rows are clearly visible, and align along the  $A$  and  $B$  directions. The two directions cross each other at an angle of  $71\pm 2^\circ$ . More details of the internal structure, orientation, and packing arrangement of the adlayer and individual complexes are revealed in a high-resolution STM image shown in Figure 2b. The molecular appearance of the complex is clearly different from that of its ligand BPMB shown in Fig-

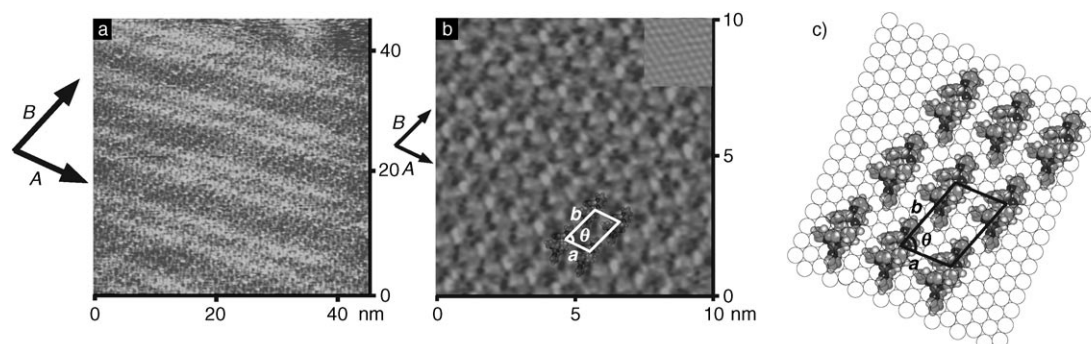


Figure 2. a) Large-scale STM image of BPMB/ $\text{Zn}^{\text{II}}$  complexes adsorbed onto Au(111). b) High-resolution STM image of the BPMB/ $\text{Zn}^{\text{II}}$  complex adlayer in (a). Imaging conditions:  $E=550$  mV,  $E_{\text{tip}}=418$  mV,  $I_{\text{tip}}=1.678$  nA. The insert in the upper right corner of (b) shows an Au(111)-(1 × 1). c) Proposed structural model for the BPMB/ $\text{Zn}^{\text{II}}$  adlayer.

ure 1a. The orientation of the Au(111) substrate can be deduced from the reconstructed lines and the substrate lattice. The insert in the upper right corner of Figure 2b shows an Au(111)-(1×1) structure. Compared with the underlying Au(111) lattice, the molecular rows in the *A* direction are parallel to the ⟨121⟩ direction. The intermolecular distances *a* and *b* in the *A* and *B* directions are  $1.0 \pm 0.1$  and  $1.5 \pm 0.1$  nm (about  $2\sqrt{3}$  and  $2\sqrt{7}$  times the underlying lattice), respectively. On the basis of the orientation and intermolecular distances, the adlayer can be defined as a  $(2\sqrt{3} \times 2\sqrt{7})$  structure. The chemical structure shown in Scheme 1 suggests that the complex has a stereoscopic helical conformation. However, careful observation revealed that the complex does not assume the orientation on the Au(111) surface shown in Scheme 1. The molecules almost lie down on the substrate upon adsorption. A schematic illustration outlined in Figure 2b shows that the helical conformation is preserved and an almost flat-lying orientation is confirmed. It is known that the substrate plays an important role in the adsorption of molecules onto a solid surface. Here, the adsorption of the stereoscopic helical complex is dominated by the underlying lattice. The helix exists in the stable array with its molecular plane inclining towards the substrate. If the molecule assumes a vertical orientation on the surface, only the edges of the two pyrrole rings make contact with the substrate, resulting in an unstable adsorption. On the other hand, if the molecule adsorbs onto the surface in an almost flat-lying orientation, larger overlapping between molecules and the Au(111) surface can be achieved, resulting in a stable adlayer. Therefore, the orientation of each complex molecule can be determined and illustrated in Figure 2b. The length of a complex was measured to be  $1.6 \pm 0.1$  nm, consistent with its chemical structure.<sup>[7a]</sup> From the features shown in the images and the period of the molecular arrangement, a unit cell was determined, as outlined in Figure 2b.

A structural model for the BPMB/Zn<sup>II</sup> adlayer is proposed in Figure 2c. In this model, each helix adsorbs onto

Au(111) with its molecular plane inclining towards the surface. The appearance of the complex in the STM image is consistent with the molecular structure. The adlayer symmetry of the complex is different from that of its ligand. In this adsorption mode, a stronger overlapping between the complex and the Au(111) surface is possible.

**BPMmB ligand:** We also studied the adlayers of another ligand and complex pair, BPMmB and BPMmB/Zn, and the structural differences in their self-assemblies. The chemical structure of ligand BPMmB suggests that it can coordinate with Zn<sup>II</sup> ions to form a complex with triangular conformation.<sup>[7b]</sup> Figure 3a is a typical large-scale STM image obtained at 510 mV in an area of 30 nm × 30 nm. Similar to BPMB, the BPMmB ligands form a long-range ordered adlayer on the surface with molecular rows extending in the *A* and *B* directions, crossing each other at an angle of  $79 \pm 2^\circ$ . The rows in the *A* direction align along the ⟨121⟩ direction of the underlying Au(111). A high-resolution STM image for the BPMmB adlayer is shown in Figure 3b. Each ligand is clearly recognizable as a linear conformation composed of five discrete spots in a set, as indicated by the five solid ellipses. These bright spots are attributable to the high electron densities of two Schiff-bases, one benzene ring, and two carboxylate groups of the molecule. An STM image showing an Au(111)-(1×1) structure is inserted in the upper right corner of Figure 3b. From the (1×1) structure, the orientation and dimension of the adlayer unit cell can be easily determined. The length of each individual ligand was measured to be  $2.3 \pm 0.1$  nm, consistent with the optimized size of BPMmB. From the features of the image and the chemical structure, the molecular plane of each ligand is proposed to be parallel to the Au(111) surface. The intermolecular distances *a* and *b* in the *A* and *B* directions were measured to be  $2.0 \pm 0.1$  and  $1.3 \pm 0.1$  nm, respectively. On the basis of the adlayer orientation and intermolecular distances, a unit cell was determined, as shown in Figure 3b. The lattice constants were found to be *a* = 2.0 nm (about

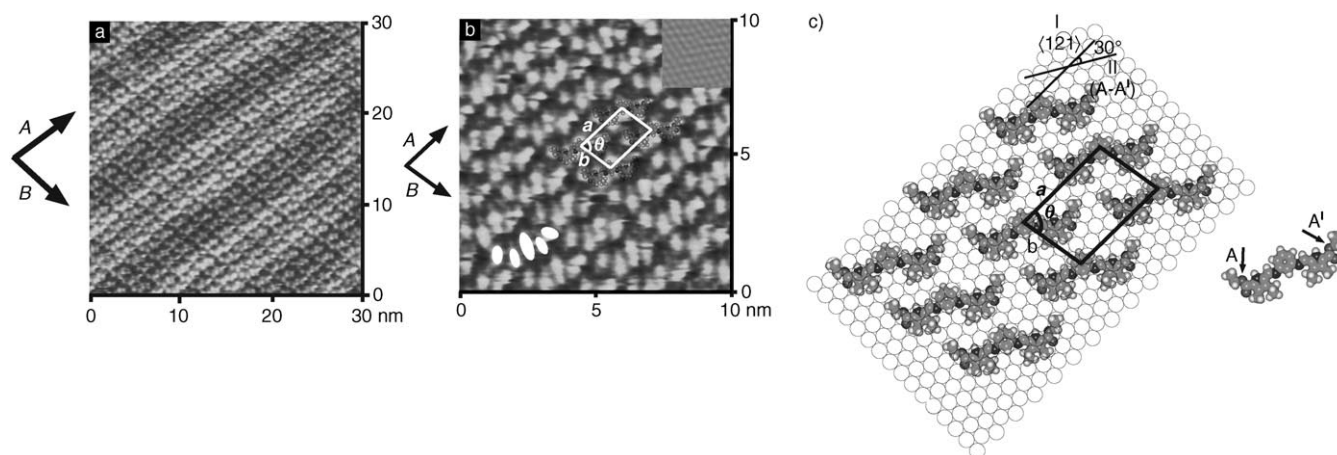


Figure 3. a) Large-scale STM image of BPMmB ligands adsorbed onto Au(111). b) High-resolution STM image of the BPMmB adlayer in (a). Imaging conditions:  $E = 510$  mV,  $E_{\text{tip}} = 379$  mV,  $I_{\text{tip}} = 556.7$  pA. The insert in the upper right corner of (b) shows an Au(111)-(1×1). c) Proposed structural model for the BPMmB adlayer.

$4\sqrt{3}$  times that of the underlying lattice) and  $b=1.3$  nm (about  $\sqrt{21}$  times that of the underlying lattice). The crossing angle is  $79^\circ$ . Therefore, the observed adlayer has a  $(4\sqrt{3}\times\sqrt{21})$  structure.

A proposed model for the observed adlayer is shown in Figure 3c. All the ligands are proposed to adsorb onto the surface in a parallel orientation and to form a self-organized adlayer with a  $(4\sqrt{3}\times\sqrt{21})$  symmetry. The benzene and pyrrole rings adsorb onto the three-fold and quasi-top site of the underlying lattice, respectively. In this arrangement, the nitrogen atoms in pyrrole rings occupy the top sites of the Au(111) substrate. Consequently, the carboxylate groups occupy these same positions, although the exact bonds to the Au(111) lattice are not clear. To explain the adsorption, two markers A and A' indicate two oxygen atoms in ethoxy units of a BPMmB molecule. Each molecule adsorbs onto the substrate along the II (A–A') direction, crossing the direction I ( $\langle 121 \rangle$  direction of the lattice) at an angle of  $30^\circ$ . This tentative model is consistent with the results of STM observations.

**BPMmB/Zn<sup>II</sup> complex:** By employing STM, we obtained direct structural evidence and detected the self-assembled architecture of BPMmB/Zn<sup>II</sup> molecules on the Au(111) surface. The STM procedures were the same as those described above. Figure 4a shows a typical large-scale STM image of the adlayer of this complex. The complexes form a well-ordered two-dimensional array with regularly molecular rows. The molecular rows aligned in the A and B directions, which are parallel to the  $\langle 121 \rangle$  direction of the underlying Au(111) lattice. The molecular rows in the two directions cross each other at an angle of  $60^\circ$ . Even in the relatively large area of  $50\text{ nm}\times 50\text{ nm}$ , individual complex molecules can be clearly observed. The image was observed consistently and was reproducible under the imaging conditions described. Details of the complex are revealed in Figure 4b, which is a high-resolution STM image acquired from the area shown in Figure 4a. The adlayer consists of sets of triangular-shaped protrusions, each with a dark depression in the center. Each complex is seen to be a triangle, consistent

with its chemical structure, and this is represented by a white solid triangle superimposed on the image. All three edges of the triangle have a length of  $1.8\pm 0.1$  nm, consistent with the crystallographic data.<sup>[7b]</sup> The results indicate that the molecular plane of the complex is parallel to the underlying Au(111) surface. The intermolecular distances  $a$  and  $b$  in both the A and B directions are around  $2.0\pm 0.1$  nm. One apex of a triangular complex is adjacent to an edge of the next complex in rows along the A direction. All the complexes self-organize into a close-packed hexagonal assembly. From the intermolecular distance and adlayer orientation, a unit cell was deduced, as shown in Figure 4b. The adlayer can be defined as a  $(4\sqrt{3}\times 4\sqrt{3})$  structure.

On the basis of these observations, a structural model for the Zn<sup>II</sup>-coordinated BPMmB complex adlayer is proposed in Figure 4c. Each complex preserves its triangular conformation on the Au(111) with a flat-lying orientation. In this arrangement, the strongest overlapping between the complex and the substrate is achieved. The intramolecular structure of the complex is consistent with that revealed by high-resolution STM images. We observed a self-organized assembly and triangular conformation of this complex, which provides direct evidence for its chemical structure.

It is known that the structures of self-assembled adlayers on solid surfaces are dependent on the subtle balance between intermolecular and molecule–substrate interactions. All ligands and complexes studied in this work self-organize into well-ordered assemblies with defined structures on a Au(111) surface. Although the ligands are the main components of their coordinated complexes, the self-assembly symmetries of the ligands and complexes are totally different, due to their different molecular conformations. The two ligands, BPMB and BPMmB, adsorb on the underlying substrate with their molecular planes parallel to the substrate surface. The complexes coordinated by Zn<sup>II</sup> ions also bind on Au(111) and form a stable adlayer. Both ligands and complexes are inclined to overlap strongly with the substrate surface. However, the adlayer structures between the ligands and related complexes are not comparable. The complex with stereoscopic helical conformation adopts a strong over-

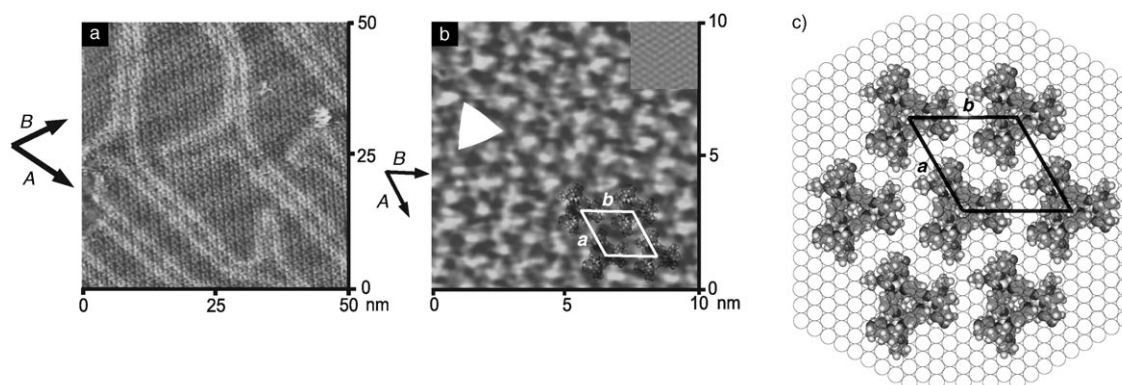


Figure 4. a) Large-scale STM image of BPMmB/Zn<sup>II</sup> complexes adsorbed onto Au(111). b) High-resolution STM image of the BPMmB/Zn<sup>II</sup> complex adlayer in (a). Imaging conditions:  $E=536$  mV,  $E_{\text{tip}}=334$  mV,  $I_{\text{tip}}=984.6$  pA. The insert in the upper right corner of (b) shows an Au(111)–(1×1). c) Proposed structural model for the BPMmB/Zn<sup>II</sup> adlayer.

lapping adsorption mode between molecule and substrate. For the complex in triangular conformation, the molecule assumes a parallel orientation of its molecular plane to the Au(111) surface. In this model, the molecule will adopt a more stable adsorption and have a larger contacting area with the Au(111) surface. On the other hand, the intermolecular interactions are usually related to molecular conformation, so that the adlayer of the triangles appears in a hexagonal network. Therefore, we can conclude that molecular conformation plays a key role in self-organization. Although the crystallographic features of the substrate will dominate the adlayer symmetry, molecular conformation is important in the adsorption of different complex molecules onto the same substrate. Here, the molecular rows are found to align in the same direction along  $\langle 121 \rangle$  in the adlayers of ligands and complexes. However, no direct relationship exists between the adsorption sites in the two pairs of adlayers.

After obtaining the well-ordered adlayers of ligands and complexes, we attempted to investigate the in-situ coordination of ligand to complex. Unfortunately, this proved to be difficult; however, experiments are still ongoing.

In summary, ligands of BPMB and BPMmB, and their  $Zn^{II}$ -coordinated complexes, were employed to prepare surface supramolecular adlayers. These molecules self-organize into well-ordered assemblies on a Au(111) substrate. The molecular conformation is responsible for the formation of the structurally defined adlayers. Although no direct relationship exists between the formation of adlayers of ligands and their complexes, all are inclined to adsorb onto the underlying substrate surface so that overlapping is optimized and a stable adlayer is formed. These results may be helpful for fabricating surface supramolecular structures and should provide insight into other research fields, such as nanotechnology and biological organization.

## Experimental Section

A well-defined Au(111) surface was prepared as described previously.<sup>[3c,8]</sup> An Au(111) facet formed on a single-crystal bead was used directly for STM observations. Before each measurement, the Au(111) electrode was annealed further in a hydrogen–oxygen flame and quenched in ultrapure water (Milli-Q,  $\geq 18.2\text{ M}\Omega$ , TOC < 5 ppb) saturated with hydrogen.

The ligands and their  $Zn^{II}$  complexes were synthesized and purified by using the method reported.<sup>[7]</sup> Spectroscopy-grade ethanol (Acros Organics) was used as solvent without further purification. The self-assemblies of both ligands and complexes were prepared by immersing the gold bead into ethanol solutions containing either  $10^{-5}\text{ M}$  ligands or their  $Zn^{II}$ -coordinated complexes for about 1 min, then taking the sample from the solution and rinsing it thoroughly with Milli-Q water. STM was carried out by using a Nanoscope E (Digital Instruments) electrochemical STM apparatus in  $0.1\text{ M HClO}_4$  (ultrapure grade from Kanto Chemical, Japan). The adlayers adsorbed onto the Au(111) surface could be protected in electrolyte solution from contamination. The electrode potentials in the STM observations were held at the double layer potential region. The typical potential used in the experiment was  $\sim 500\text{--}550\text{ mV}$  (vs RHE), at which no surface redox reaction takes place and molecular adlayers were well preserved. The STM tips were prepared by electrochemically etching a tungsten wire (0.25 mm in diameter) in  $0.6\text{ M KOH}$  with a voltage of  $\sim 12\text{--}15\text{ V}$  until the etching process stopped. The W tips were coated with

clear nail polish to minimize the Faradic current. STM images were recorded in the constant-current mode by using a high-resolution scanner (HD-2140A). Tunneling conditions are reported in the corresponding figure captions. The molecular models were constructed according to the crystallographic data and optimized by the AM1 method in HyperChem 6.0 (Hypercube). The numerical values for the molecules were estimated from the molecular models.

## Acknowledgements

This work was supported by the National Natural Science Foundation of China (Nos. 20025308 and 20177025), National Key Project on Basic Research (Grants G2000077501 and 2002CCA03100), and the Chinese Academy of Sciences. The authors thank Lan-Ying Yang, Zhi-Kun Wu, and Jin-Shi Ma for kindly providing us samples.

- [1] a) C. Piguët, G. Bernardinelli, G. Hopfgartner, *Chem. Rev.* **1997**, *97*, 2005–2062; b) S. Leininger, B. Olenyuk, P. J. Stang, *Chem. Rev.* **2000**, *100*, 853–907; c) G. F. Swieggers, T. J. Malefsete, *Chem. Rev.* **2000**, *100*, 3483–3537; d) M. Eddaoudi, D. B. Moler, H. L. Li, B. L. Chen, T. M. Reineke, M. O’Keeffe, O. M. Yaghi, *Acc. Chem. Res.* **2001**, *34*, 319–330; e) S. R. Seidel, P. J. Stang, *Acc. Chem. Res.* **2002**, *35*, 972–983; f) P. S. Mukherjee, N. Das, P. J. Stang, *J. Org. Chem.* **2004**, *69*, 3526–3529; g) C. A. Schalley, *J. Phys. Org. Chem.* **2004**, *17*, 967–972; h) C. Addicott, N. Das, P. J. Stang, *Inorg. Chem.* **2004**, *43*, 5335–5338; i) I. M. Müller, D. Möller, C. A. Schalley, *Angew. Chem.* **2005**, *117*, 485–488; *Angew. Chem. Int. Ed.* **2005**, *44*, 480–484; j) B. Hasenknopf, J. M. Lehn, N. Boumediene, A. Dupont-Gervais, A. van Dorselaer, B. Kneisel, D. Fenske, *J. Am. Chem. Soc.* **1997**, *119*, 10956–10962.
- [2] a) P. F. H. Schwab, M. D. Levin, J. Michl, *Chem. Rev.* **1999**, *99*, 1863–1933; b) B. J. Holliday, C. A. Mirkin, *Angew. Chem.* **2001**, *113*, 2076–2097; *Angew. Chem. Int. Ed.* **2001**, *40*, 2022–2043; c) F. A. Cotton, C. Lin, C. A. Murillo, *Acc. Chem. Res.* **2001**, *34*, 759–771; d) D. L. Caulder, K. N. Raymond, *Acc. Chem. Res.* **1999**, *32*, 975–982; e) M. Fujita, *Chem. Soc. Rev.* **1998**, *27*, 417–425; f) P. J. Stang, B. Olenyuk, *Acc. Chem. Res.* **1997**, *30*, 502–518; g) F. A. Cotton, C. Lin, C. A. Murillo, *Proc. Natl. Acad. Sci. USA* **2002**, *99*, 4810–4813; h) M. Eddaoudi, J. Kim, D. Vodak, A. Sudik, J. Wachter, M. O’Keeffe, O. M. Yaghi, *Proc. Natl. Acad. Sci. USA* **2002**, *99*, 4900–4904; i) L. Pirondini, F. Bertolini, B. Cantadori, F. Uguzzoli, C. Massera, E. Dalcanales, *Proc. Natl. Acad. Sci. USA* **2002**, *99*, 4911–4915; j) C. J. Kuehl, Y. K. Kryschenko, U. Radhakrishnan, S. R. Seidel, S. D. Huang, P. J. Stang, *Proc. Natl. Acad. Sci. USA* **2002**, *99*, 4932–4936; k) P. H. Dinolfo, J. T. Hupp, *Chem. Mater.* **2001**, *13*, 3113–3125; l) F. Würthner, C. C. You, C. R. Saha-Möller, *Chem. Soc. Rev.* **2004**, *33*, 133–146.
- [3] a) J. M. Lehn, *Supramolecular Chemistry: Concepts and Perspectives*, VCH, Weinheim, **1995**; b) J. L. Atwood, J. E. D. Davies, D. D. MacNicol, F. Vögtle, J. M. Lehn, *Comprehensive Supramolecular Chemistry, Vol. 9*, Pergamon, New York, **1996**; c) J. R. Gong, L. J. Wan, Q. H. Yuan, C. L. Bai, H. Jude, P. J. Stang, *Proc. Natl. Acad. Sci. USA* **2005**, *102*, 971–974; d) B. D. Gates, Q. B. Xu, M. Stewart, D. Ryan, C. G. Willson, G. M. Whitesides, *Chem. Rev.* **2005**, *105*, 1171–1196; e) S. De Feyter, F. C. De Schryver, *J. Phys. Chem. B* **2005**, *109*, 4290–4302.
- [4] a) Q. M. Xu, D. Wang, L. J. Wan, C. Wang, C. L. Bai, G. Q. Feng, M. X. Wang, *Angew. Chem.* **2002**, *114*, 3558–3561; *Angew. Chem. Int. Ed.* **2002**, *41*, 3408–3411; b) W. L. Deng, K. W. Hipps, *J. Phys. Chem. B* **2003**, *107*, 10736–10740; c) K. Suto, S. Yoshimoto, K. Itaya, *J. Am. Chem. Soc.* **2003**, *125*, 14976–14977; d) S. M. Xu, G. Szymanski, J. Lipkowski, *J. Am. Chem. Soc.* **2004**, *126*, 12276–12277; e) D. M. Kolb, *Angew. Chem.* **2001**, *113*, 1198–1220; *Angew. Chem. Int. Ed.* **2001**, *40*, 1162–1181; f) C. Safarowsky, L. Merz, A. Rang, P. Broekmann, B. A. Hermann, C. A. Schalley, *Angew. Chem.* **2004**, *116*, 1311–1314; *Angew. Chem. Int. Ed.* **2004**, *43*, 1291–1294.
- [5] a) T. Suzuki, K. Nakashima, S. Shinkai, *Chem. Lett.* **1994**, 469–472; b) G. B. Pan, J. M. Liu, H. M. Zhang, L. J. Wan, Q. Y. Zheng, C. L.

- Bai, *Angew. Chem.* **2003**, *115*, 2853–2857; *Angew. Chem. Int. Ed.* **2003**, *42*, 2747–2751.
- [6] a) A. Semenov, J. P. Spatz, M. Möller, J. M. Lehn, B. Sell, D. Schubert, C. H. Weidl, U. S. Schubert, *Angew. Chem.* **1999**, *111*, 2701–2705; *Angew. Chem. Int. Ed.* **1999**, *38*, 2547–2550; b) U. Ziener, J. M. Lehn, A. Mourran, M. Möller, *Chem. Eur. J.* **2002**, *8*, 951–957; c) D. G. Kurth, N. Severin, J. P. Rabe, *Angew. Chem.* **2002**, *114*, 3833–3835; *Angew. Chem. Int. Ed.* **2002**, *41*, 3681–3683; d) Q. M. Xu, B. Zhang, L. J. Wan, C. Wang, C. L. Bai, D. B. Zhu, *Surf. Sci.* **2002**, *517*, 52–58; e) H. Spillmann, A. Dmitriev, N. Lin, P. Messina, J. V. Barth, K. Kern, *J. Am. Chem. Soc.* **2003**, *125*, 10725–10728; f) D. L. Shieh, K. B. Shiu, J. L. Lin, *Surf. Sci.* **2004**, *548*, L7–L12; g) N. Lin, A. Dmitriev, J. Weckesser, J. V. Barth, K. Kern, *Angew. Chem.* **2002**, *114*, 4973–4977; *Angew. Chem. Int. Ed.* **2002**, *41*, 4779–4783; h) E. Figge-meier, L. Merz, B. A. Hermann, Y. C. Zimmermann, C. E. House-croft, H. J. Guntherodt, E. C. Constable, *J. Phys. Chem. B* **2003**, *107*, 1157–1162; i) S. Stepanow, M. Lingenfelder, A. Dmitriev, H. Spillmann, E. Delvigne, N. Lin, X. B. Deng, C. Z. Cai, J. V. Barth, K. Kern, *Nat. Mater.* **2004**, *3*, 229–233; j) S. De Fetyer, M. M. S. Abdel-Mottaleb, N. Schuurmans, B. J. V. Verkuil, J. H. van Esch, B. L. Feringa, F. C. De Schryver, *Chem. Eur. J.* **2004**, *10*, 1124–1132; k) M. A. Lingenfelder, H. Spillmann, A. Dmitriev, S. Stepanow, N. Lin, J. V. Barth, K. Kern, *Chem. Eur. J.* **2004**, *10*, 1913–1919; l) S. Takaishi, H. Miyasaka, K. Sugiura, M. Yamashita, H. Matsuzaki, H. Kishida, H. Okamoto, H. Tanaka, K. Marumoto, H. Ito, S. Kuroda, T. Takami, *Angew. Chem.* **2004**, *116*, 3233–3237; *Angew. Chem. Int. Ed.* **2004**, *43*, 3171–3175; m) A. Dmitriev, H. Spillmann, M. Lingenfelder, N. Lin, J. V. Barth, K. Kern, *Langmuir* **2004**, *20*, 4799–4801; n) P. Zell, F. Mögele, U. Ziener, B. Rieger, *Chem. Commun.* **2005**, 1294–1296; o) N. Lin, S. Stepanow, F. Vidal, J. V. Barth, K. Kern, *Chem. Commun.* **2005**, 1681–1683; p) N. Kakegawa, N. Hoshino, Y. Matsuo-ka, N. Wakabayashi, S. I. Nishimura, A. Yamagishi, *Chem. Commun.* **2005**, 2375–2377; q) S. Stepanow, N. Lin, F. Vidal, A. Landa, M. Ruben, J. V. Barth, K. Kern, *Nano Lett.* **2005**, *5*, 901–904; r) P. Qian, H. Nanjo, N. Sanada, T. Yokoyama, T. M. Suzuki, *Chem. Lett.* **2000**, 1118–1119; s) A. Mourran, U. Ziener, M. Möller, E. Breuning, M. Ohkita, J. M. Lehn, *Eur. J. Inorg. Chem.* **2005**, *13*, 2641–2647.
- [7] a) L. Y. Yang, Q. Q. Chen, G. Q. Yang, J. S. Ma, *Tetrahedron* **2003**, *59*, 100037–100041; b) Z. Wu, Q. Chen, S. Xiong, B. Xin, Z. Zhao, L. Jiang, J. S. Ma, *Angew. Chem.* **2003**, *115*, 3393–3396; *Angew. Chem. Int. Ed.* **2003**, *42*, 3271–3274.
- [8] L. J. Wan, M. Terashima, H. Noda, M. Osawa, *J. Phys. Chem. B* **2000**, *104*, 3563–3569.

Received: July 19, 2005  
Published online: January 19, 2006